

The computer application for the mathematical modeling of optical fibers used in metrology based on Newton polynomial interpolation

Abstract. This paper proposes an original application enabling the design of single mode and multimode optical fibers of selected refractive index profiles. It can be used to determine the parameters of optical fibers used in the construction of optical sensors and measuring converters, as well as optical fiber telemetry systems. The developed application uses in its operation a set of mathematical formulas available in scientific studies, as well as Newton polynomial interpolation. They have been presented and discussed in this study to demonstrate the suitability of the application in determining the values of parameters such as: molar concentration of germanium GeO_2 in the core, Verdet constant, refractive index in the core and cladding, cutoff wavelength. Tests of the developed application were carried out for telecommunications fibers commonly available and used in metrology (single mode and multimode). The obtained results were compared with the generally available test results of these fibers. This allowed for the formulation of conclusions regarding the accuracy of the calculations performed by the application and the correctness of its operation.

Streszczenie. W artykule zaproponowano autorską aplikację umożliwiającą projektowanie światłowodów jednomodowych i wielomodowych o wybranych profilach współczynnika załamania światła. Może ona służyć do wyznaczania parametrów światłowodów wykorzystywanych do budowy optycznych czujników i przetworników pomiarowych, a także światłowodowych systemów telemetrycznych. Opracowana aplikacja wykorzystuje w swoim działaniu zestaw wzorów matematycznych dostępnych w opracowaniach naukowych, a także interpolację wielomianową Newtona. Zostały one przedstawione i omówione w niniejszej pracy w celu wykazania przydatności aplikacji do wyznaczania wartości parametrów takich jak: stężenie molowe germanu GeO_2 w rdzeniu światłowodu, stała Verdet, współczynnik załamania światła w rdzeniu i płaszczu, długość fali odcięcia. Testy opracowanej aplikacji przeprowadzono dla światłowodów telekomunikacyjnych (jednomodowych i wielomodowych) powszechnie dostępnych i stosowanych w metrologii. Uzyskane wyniki porównano z ogólnie dostępnymi wynikami badań tych włókien. Pozwoliło to na sformułowanie wniosków dotyczących dokładności obliczeń wykonywanych przez aplikację oraz poprawności jej działania. (**Komputerowa aplikacja do matematycznego modelowania włókien światłowodowych stosowanych w metrologii wykorzystująca interpolację wielomianową Newtona**)

Keywords: application for designing and visualizing optical fibers, Newton polynomial interpolation, optical fiber sensor and measuring transducer, measurements of electrical and non-electrical quantities, photosensitive fibers

Słowa kluczowe: aplikacja do projektowania i wizualizacji światłowodów, interpolacja wielomianowa Newtona, światłowodowy czujnik i przetwornik pomiarowy, pomiary wielkości elektrycznych i nieelektrycznych, włókna fotouczulone

Introduction

The first records of using optical fibers in metrology date back to the 1980s [1]. However, the following years brought stagnation, which could be caused by high costs of the sensor implementation compared to a classic current transformer and the lack of appropriate optical fibers. Return to work on the issue of optical fiber sensors can be observed from the end of the 1990s [2]. The active element of the sensor can be an optical fiber [1,3,4,5] through which laser light propagates. At the same time, work began on the possibility of using optical fibers in telemetry systems [6].

The issues of designing and using optical fibers in metrology are currently very popular and are the subject of theoretical and experimental research [7,8,9,10,11,12]. It should be added here that there are also studies on the design of single mode and multimode telecommunication optical fibers for other purposes, with particular emphasis on the effect of the light wavelength and the molar concentration of the GeO_2 impurity in the core of this type of fiber on the metrological properties of sensors and the possibility of their use in remote systems measurement, control, and protection.

The biggest problem occurring during the construction of sensors and measuring transducers of electrical and non-electrical quantities using optical fiber technology is to obtain high processing sensitivity. Based on many scientific studies, it can be stated, that doping the optical fiber core with rare earth elements – neodymium (Nd) either holmium (Ho) [7,8] significantly improves the processing sensitivity of optical fiber sensor. However, these optical fibers are very expensive and they limit the length of the optical fiber sensor either transducers.

This article focuses primarily on single mode telecommunications optical fiber used to build optical fiber telemetry systems [6], optical fiber transducers “electric current – the angle of rotation of the plane of polarization of light” [9,10,11], “electric current – attenuation depends of polarization” [12] and also multimode telecommunications optical fibers used for construction distributed temperature sensors, which use the forced Raman scattering [5]. This is due to the availability and affordable price of these fibers, in relation to optical fibers doped with rare earth elements. On these examples, the usefulness of the presented application for designing optical fibers used in metrology has been demonstrated.

Characteristics of the application enabling the design of optical fiber used in metrology

TOFMA (Telecommunications Optical Fibers Modeling Applications) is the computer application created for the design of single mode and multimode optical fibers used in the metrology of electrical and non-electrical quantities.

It consists of two subpages: main and application. The main subpage has: a menu with links, contact to the authors, licenses and bibliography. To use the application, go to the Application subpage via the menu (Fig. 1.).

This application makes it possible to determine the refractive index in the core, cladding and depression (if present) of the optical fiber; Verdet constant in the core, cladding and depression (if present) of the optical fiber and the cutoff wavelength. Additionally, two-dimensional (2D) or three-dimensional (3D) plots of changes of the refractive index can be generated depending on the distance from the center of the core of the considered optical fiber.

To do this, select one of five consecutively numbered profiles (Fig. 2.). Then enter the necessary values for calculations (fields that do not participate in calculations for a given profile are automatically excluded and marked in gray).

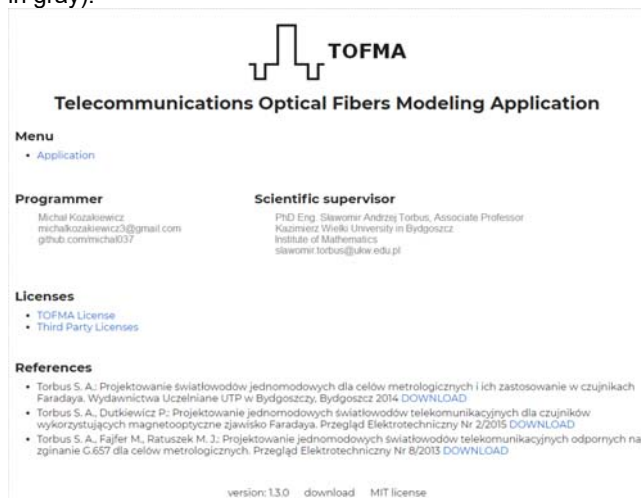


Fig. 1. Screenshot of the main page of the TOFMA application

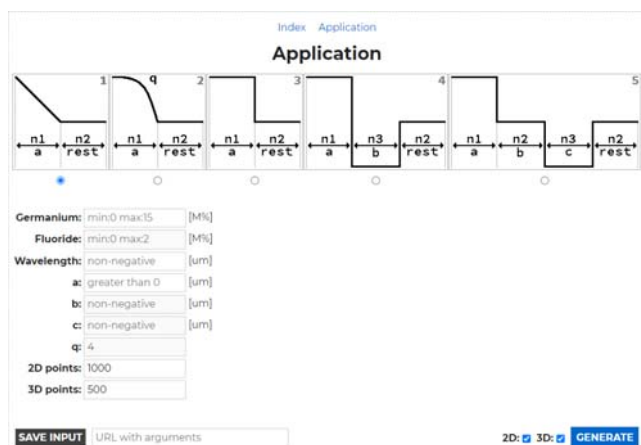


Fig. 2. Screenshot of the application subpage: **1** – triangular profile, **2** – gradient profile, **3** – step profile, **4** – step profile with a depressive cladding, **5** – step profile with a depressive ring around the core, **Germanium** – molecular concentration of germanium in the optical fiber core (from 0,0 M% to 13,5 M%), **Fluoride** – molar concentration of fluorine in the depressive cladding (from 0,0 M% to 2,0 M%), **Wavelength** – length of the propagated light wave in the optical fiber core, **a** – radius of the optical fiber core, **b** – width of the cladding depression (in the case of profile 4) or the distance between the core and the depressive ring around the core (in the case of profile 5), **c** – the width of the depressive ring around the cladding (in the case of profile 5), **q** – gradient correction parameter (in the case of profile 2), **2D points** – number of points for the two-dimensional plot, **3D points** – number of points for the three-dimensional plot

After entering the relevant data, you must confirm it by pressing the GENERATE button. Appropriate calculations and generated plots will then be carried out.

The algorithms of calculations are based on the theory contained in the works [18]. This means that the index of refraction in the glass from which the components of the optical fiber are made is calculated from the Sellmeier equation [13,14]:

$$(1) \quad n^2 = 1 + \frac{a_1 \cdot \lambda^2}{\lambda^2 - b_1^2} + \frac{a_2 \cdot \lambda^2}{\lambda^2 - b_2^2} + \frac{a_3 \cdot \lambda^2}{\lambda^2 - b_3^2}$$

where: a_i – constant, b_i – constant [μm], λ – wavelength [μm]. Values of coefficients in equation (1) for strictly defined values of molar concentration of germanium or fluorine admixture have been tabulated (Table 1. and Table 2.).

Table 1. Coefficients a_i and b_i occurring in formula (1) for pure SiO_2 and selected germanium molar concentrations [13]

Sellmeier equation coefficients	0,0 M% pure SiO_2	Molecular concentration of germanium admixture in the optical fiber core			
		3,1 M%	5,8 M%	7,9 M%	13,5 M%
a_1	0,6961663	0,7028554	0,7088876	0,7136824	0,711040
a_2	0,4079426	0,4146307	0,4206803	0,4254807	0,451885
a_3	0,8974994	0,8974540	0,8956551	0,8964226	0,704048
b_1	0,0684043	0,0727723	0,0609053	0,0617167	0,064270
b_2	0,1162414	0,1143085	0,1254514	0,1270814	0,129408
b_3	9,8961610	9,8961610	9,8961620	9,8961610	9,425478

Table 2. Coefficients a_i and b_i occurring in formula (1) for pure SiO_2 and selected fluorine molar concentrations [13]

Sellmeier equation coefficients	The molar concentration of fluorine in the optical fiber cladding		
	0,0 M% pure SiO_2	1,0 M%	2,0 M%
a_1	0,6961663	0,69325	0,67744
a_2	0,4079426	0,39720	0,40101
a_3	0,8974994	0,86008	0,87193
b_1	0,0684043	0,06724	0,06135
b_2	0,1162414	0,11714	0,12030
b_3	9,8961610	9,77610	9,85630

Lagrange polynomial interpolation [15] is widely known and used, because it is more efficient when several datasets need to be interpolated on the same data points. Newton polynomial interpolation is more efficient when you have to interpolate data incrementally.

The application uses Newton polynomial interpolation [15] fifth degree for germanium and third degree for fluorine. This is due to the fact, that the Lagrange method is mostly a theoretical tool used for proving theorems. Additionally, it is not very efficient when a new point is added (which requires computing the polynomial again, from scratch), it is also numerically unstable. These disadvantages are eliminated by Newton's method, which is a variation of the Lagrange interpolation, which is numerically stable and computationally efficient.

The interpolation makes it possible to determine the values of the Sellmeier equation coefficients (1) for any values of molar concentrations of germanium (from 0,0 M% to 13,5 M%) and admixture of fluorine (from 0,0 M% to 2,0 M%).

For profile 1 (triangular) and 2 (gradient), the distribution of the refractive index is determined based on the dependence [16]:

$$(2) \quad n^2(R) = \begin{cases} n_1^2 \cdot (1 - 2 \cdot \Delta \cdot R^q) & \text{dla } 0 \leq R < 1 \\ n_2^2 = n_1^2 \cdot (1 - 2 \cdot \Delta) & \text{dla } 1 \leq R < \infty \end{cases}$$

where: $R = \frac{r}{a}$ – normalized radius, a – core radius

or characteristic dimension of the profile [μm], r – distance from the center of the core [μm], n_1 – the value of the refractive index in the core for $r = 0$ – in the center of the

core, $\Delta = \frac{n_1^2 - n_2^2}{2 \cdot n_1^2}$, n_2 – the value of the refractive index

in the cladding.

Profiles 3 (step), 4 (step with the depressive cladding) and 5 (step with the depressive ring around the core) are created by specifying specific refractive indices for specific distances from the center of the optical fiber core. This method creates a two-dimensional plot.

A three-dimensional plot is created in a similar way, for the square XY plane, the Z space containing values of the refractive index n is added. The application uses the formula for the length of a two-dimensional vector, where the constant point is the center of the XY plane.

Verdet constant, of which fiber components are made, is calculated using the following formulas [17,18]:

$$(3) \quad V = \frac{1}{2} \cdot \frac{e}{m_e} \cdot \frac{\lambda}{c} \cdot \left| \frac{\partial n}{\partial \lambda} \right| \left[\frac{\text{rad}}{\text{T} \cdot \text{m}} \right]$$

$$(4) \quad \frac{\partial n}{\partial \lambda} = - \frac{\sum_{i=1}^3 \frac{a_i \cdot b_i^2 \cdot \lambda}{(\lambda^2 - b_i^2)^2}}{\sqrt{1 + \sum_{i=1}^3 \frac{a_i \cdot \lambda^2}{\lambda^2 - b_i^2}}} \left[\frac{1}{\mu\text{m}} \right]$$

where: e/m – the right charge of the electron ($1,7588200107721635 \cdot 10^{11}$ C/kg), λ – wavelength [μm], c – speed of light in a vacuum ($c = 2,99792458 \cdot 10^8$ m/s), $\left| \frac{\partial n}{\partial \lambda} \right|$ – the absolute value of the refractive index change relative to the wavelength $1/\text{m}$.

The cut-off wavelength is determined based on the dependence [13,16]:

$$(5) \quad \lambda_c = \frac{2 \cdot \pi \cdot a}{V_c} \cdot NA \quad [\mu\text{m}]$$

where: a – the radius of the optical fiber core or the characteristic dimension of the profile [μm],

$NA = n_1 \cdot \sqrt{2 \cdot \Delta}$ – numerical aperture, $V_c = V_{c_{\infty}} \cdot \sqrt{\frac{q+2}{q}}$

– normalized frequency for the step profile with the power factor q , $V_{c_{\infty}} = 2,405$ – normalized frequency for the step profile (where $q \rightarrow \infty$).

The application is built using JavaScript language and has open source code (MIT license).

The results of the application operation on the example of selected telecommunications optical fibers

Telecommunications optical fiber (Fig. 3.) is composed of two layers of silica – SiO_2 , which are characterized by different refractive index. It is therefore a thin multilayer dielectric fiber [19,20], whose inner, centrally located layer is called the core and is covered with a tightly fitting layer called cladding. The core is characterized by a higher refractive index – n_1 than the surrounding layer – cladding with refractive index – n_2 [19,21], to be able to carry out the transmission in it by the law of total internal reflection. Additionally, there is the third layer, which is a protective coating called the primary protective layer. It gives for the fibers mechanical resistance and it protects against microcracks, to which their surface is exposed, especially when contacting other materials. This coating is applied during the fiber extraction process. The optical fiber having these three layers has a total diameter of 250 μm [19,22].

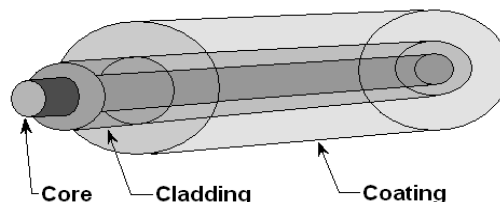


Fig. 3. Structure of telecommunication optical fiber

The basic material, which optical fibers are made of, including telecommunications, is silica SiO_2 , which should be doped in order to obtain the appropriate refractive index in the core or in the cladding. It is possible to distinguish admixtures of such elements as: borium (B), fluorum (F), aluminium (Al), phosphorus (P), germanium (Ge), thallium (Tl) and other [20,22]. Glass of the following type is used $\text{SiO}_2\text{-B}_2\text{O}_3$ and $\text{SiO}_2\text{-F}_2$, which are materials with a refractive index less by almost 1% [20,22] and glass type $\text{SiO}_2\text{-GeO}_2$, $\text{SiO}_2\text{-P}_2\text{O}_5$, $\text{SiO}_2\text{-TiO}_2$ and $\text{SiO}_2\text{-Al}_2\text{O}_3$, which increase the refractive index over 1% [20,22,23].

Telecommunications optical fibers can be divided into multimode and single mode. Mode is a monochrome beam (not a flat wave) propagating along the waveguide with the characteristic phase velocity, with characteristic transverse distribution of intensity unchanging along the direction of propagation. It means, mode propagates in the waveguide without changing the shape and with the characteristic speed [13]. In single mode telecommunications optical fibers, it propagates only one mod called the primary one and it is marked as LP_{01} (HE_{11}), side modes are strongly suppressed. However, in multimode optical fibers it propagates many mods (primary mode and additional – side modes). Different modes may differ in the shape of the field distribution and speed of propagation, therefore the value of const propagation [13]. This occurrence has a negative effect on the transmission of the optical signal, because it causes multiple signal speeds, which causes the signal to blur as it propagates with a waveguide [13]. We are dealing with this fact in multimode optical fibers, which affects the reduction of transmission speed and range. This defect has been eliminated in single mode optical fibers, which provide very high speed and a large transmission range.

Multimode and single mode optical fibers have standardized diameter of core and cladding. Depending on the optical fiber class, they are respectively [20]:

- 50 μm / 125 μm or 62,5 μm / 125 μm in the case of multimode optical fibers,
- 5 \div 11 μm / 125 μm in the case of single mode optical fibers.

Detailed characteristics of telecommunications optical fibers used in metrology, which can be designed using the created application, are included in the recommendations of the International Telecommunications Union (ITU):

- multimode optical fibers refer to the ITU-T G.651 recommendation – optical fibers of step and gradient profile of refractive index in the core, core made of glass type $\text{SiO}_2\text{-GeO}_2$ and the cladding made of pure silica SiO_2 ,
- ITU-T G.652 recommendations apply to single mode optical fibers not resistant to bending – optical fibers of step profile of refractive index in the core, core made of glass type $\text{SiO}_2\text{-GeO}_2$ and the cladding made of pure silica SiO_2 ,
- ITU-T G.653 – optical fibers with a triangular profile of refractive index in the core, core made of glass type $\text{SiO}_2\text{-GeO}_2$ and the cladding made of pure silica SiO_2 ,
- optical fibers resistant to bending refer to the ITU-T G.657 recommendation – optical fibers of step profile of

refractive index in the core, in each case the core is made of type glass $\text{SiO}_2\text{-GeO}_2$, depressive cladding, depressive ring or depressive nano ring made of type glass $\text{SiO}_2\text{-F}_2$ and the cladding made of pure silica SiO_2 .

The normalized parameters of the above-mentioned multimode optical fibers are included in Table 3. (multimode optical fibers), Table 4. (single mode optical fibers not resistant to bending) and Table 5. (single mode optical fibers resistant to bending).

It is known, that single mode telecommunications optical fibers (ITU-T G.652, G.653 and G.655) are not very resistant to bending, exhibit a significant increase of suppression depending on the bending radius. With small bending radius ($R < 55$ mm) they cannot be wound on the object being analyzed, which is a big inconvenience, because this is the method of assembly used in the case of optical fiber current sensors. In recent years, various designs of single mode telecommunications optical fibers resistant to bending have appeared on the optoelectronics market (ITU-T G.657). The best of them, with a depressive cladding, depressive ring and especially with the depressive nano ring are exhibiting suppression below 0,1 dB/loop at the radius of bending $R = 5$ mm. By this property, they can be placed directly on the analyzed object.

Table 3. Standardized parameters of multimode optical fibers used during the design [11]

Refractive index profile in the core	step (G.651)	gradient (G.651)
Diameter of the core	50,0 μm or 62,5 μm	
Molecular concentration of germanium in the core	10,5 M%	
Wavelength	0,85 μm (1 st optical window)	

Table 4. Standardized parameters of single mode optical fibers not resistant to bending used during design [9,10]

Refractive index profile in the core	step (G.652)	triangular (G.653)
Diameter of the core	8,5 μm	6,0 μm
Molecular concentration of germanium in the core	3,1 M%	7,9 M%
Wavelength	1,31 μm (2 nd optical window) 1,55 μm (3 rd optical window)	

Table 5. Standardized parameters of single mode optical fibers resistant to bending used during design [11,24]

Refractive index profile in the core	step profile with increased relative difference of refractive index and reduced core radius (G.657A)	step profile with depressive cladding (G.657B)	step profile with depressive ring around the core (G.657B)
Diameter of the core	8,6 \pm 9,5 \pm 0,4 μm	6,3 \pm 9,5 \pm 0,4 μm	
Molecular concentration of germanium in the core	3,5 M%	3,0 M%	3,0 M%
Molar concentration of fluorine in the depressive cladding	–	0,6 M%	–
Molar concentration of fluorine in the depressive ring around the core	–	–	1,0 M%
Wavelength	1,31 μm (2 nd optical window) 1,55 μm (3 rd optical window)		

Table 6. Simulation parameters and calculation results for G.651 multimode optical fiber with a gradient profile [own results]

Core radius [μm]	25,00	31,25
Wavelength [μm]	0,85	0,85
Molecular concentration of germanium in the core [M%]	10,5	10,5
Verdet constant $\left[\frac{\text{rad}}{\text{T} \cdot \text{m}} \right]$	4,2309	4,2309
The refractive index in the core	1,4692	1,4692
The refractive index in the cladding	1,4525	1,4525
Cutoff wavelength [μm]	11,8	14,7

In order to test the application, the characteristic parameters of multimode and single mode telecommunications optical fibers presented in Table 1. ÷ 3. were used. The obtained results are presented in Table 6. ÷ 11. and in Fig. 4. ÷ 9.

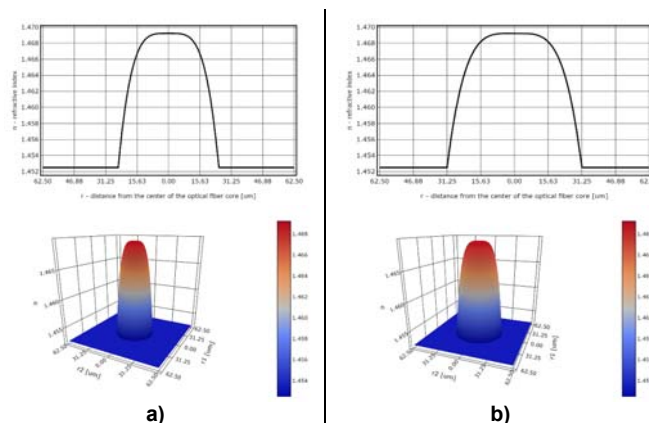


Fig. 4. The profile shapes of the refractive index in the core and the cladding of the multimode G.651 optical fiber for the 1st optical window: a) plot 2D and 3D for the core diameter of 50,0 μm , b) plot 2D and 3D for the core diameter 62,5 μm [own results]

Table 7. Simulation parameters and calculation results for G.652 single mode optical fiber with step profile [own results]

Core radius [μm]	4,25	4,25
Wavelength [μm]	1,31	1,55
Molecular concentration of germanium in the core [M%]	3,1	3,1
Verdet constant $\left[\frac{\text{rad}}{\text{T} \cdot \text{m}} \right]$	4,3814	5,4617
The refractive index in the core	1,4515	1,4487
The refractive index in the cladding	1,4468	1,4440
Cutoff wavelength [μm]	1,29	1,29

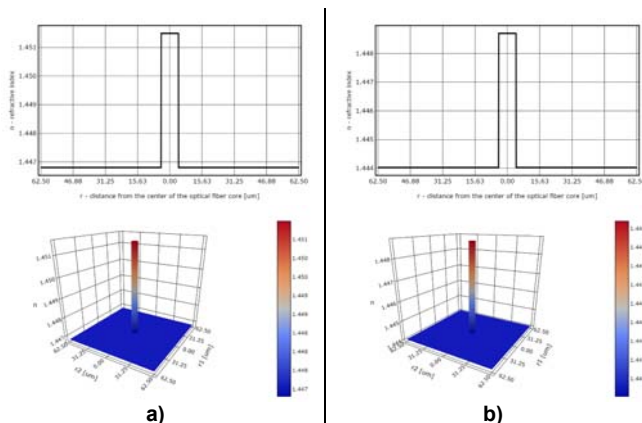


Fig. 5. The profile shapes of the refractive index profile in the core and cladding of G.652 single mode optical fiber: a) plot 2D and 3D for 2nd optical window, b) plot 2D and 3D for 3rd optical window [own results]

Table 8. Simulation parameters and calculation results for G.653 single mode optical fiber with triangular profile [own results]

Core radius [μm]	3,00	3,00
Wavelength [μm]	1,31	1,55
Molecular concentration of germanium in the core [M%]	7,9	7,9
Verdet constant $\left[\frac{\text{rad}}{\text{T} \cdot \text{m}} \right]$	4,4120	5,4680
The refractive index in the core	1,4590	1,4562
The refractive index in the cladding	1,4468	1,4440
Cutoff wavelength [μm]	0,85	0,85

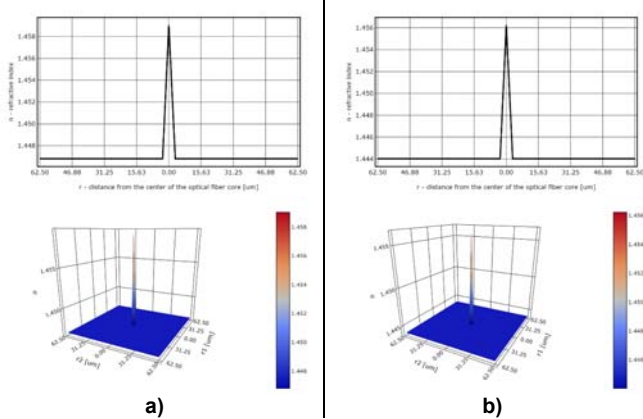


Fig. 6. The profile shapes of the refractive index profile in the core and cladding of G.653 single mode optical fiber: **a)** plot 2D and 3D for 2nd optical window, **b)** plot 2D and 3D for 3rd optical window [own results]

Table 9. Simulation parameters and calculation results for G.657A single mode optical fiber with step profile, increased relative difference in refractive index and reduced core radius [own results]

Core radius [μm]	4,10	4,10
Wavelength [μm]	1,31	1,55
Molecular concentration of germanium in the core [M%]	3,5	3,5
Verdet constant $\left[\frac{\text{rad}}{\text{T} \cdot \text{m}} \right]$	4,3758	5,4550
The refractive index in the core	1,4521	1,4493
The refractive index in the cladding	1,4468	1,4440
Cutoff wavelength [μm]	1,33	1,33

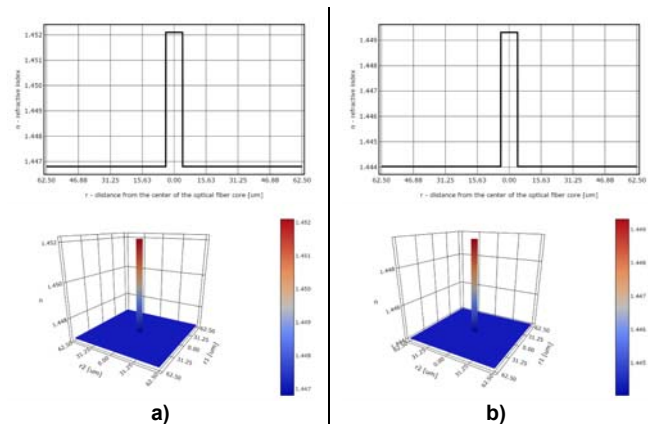


Fig. 7. The profile shapes of the refractive index in the core and the cladding of G.657A single mode optical fiber: **a)** plot 2D and 3D for 2nd optical window, **b)** plot 2D and 3D for 3rd optical window [own results]

Table 10. Simulation parameters and calculation results for G.657B single mode optical fiber with step profile and depressive cladding [own results]

Core radius [μm]	3,35	3,35
Wavelength [μm]	1,31	1,55
Molecular concentration of germanium in the core [M%]	3,0	3,0
Width of the cladding depression [μm]	3,20	3,20
Molecular concentration of fluorine in the depressive cladding [M%]	0,6	0,6
Verdet constant $\left[\frac{\text{rad}}{\text{T} \cdot \text{m}} \right]$	4,3830	5,4635
The refractive index in the core	1,4513	1,4485
The refractive index in the cladding	1,4468	1,4440
The refractive index in the cladding depression	1,4439	1,4412
Cutoff wavelength [μm]	1,00	1,00

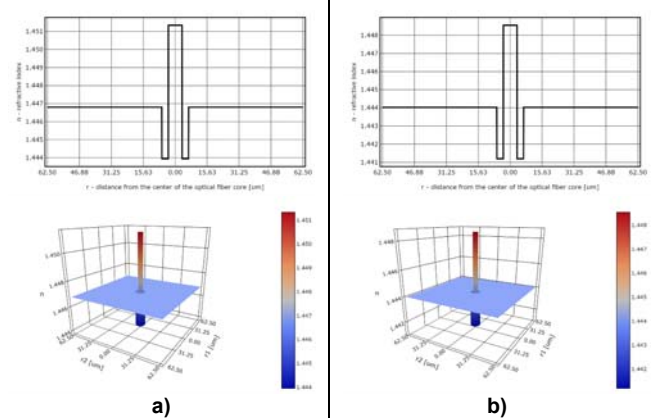


Fig. 8. The profile shapes of the refractive index in the core and the cladding of G.657B single mode optical fiber: **a)** plot 2D and 3D for 2nd optical window, **b)** plot 2D and 3D for 3rd optical window [own results]

Table 11. Simulation parameters and calculation results for G.657B single mode optical fiber with step profile and the cladding with the depressive ring around the core [own results]

Core radius [μm]	3,35	3,35
Wavelength [μm]	1,31	1,55
Molecular concentration of germanium in the core [M%]	3,0	3,0
Width of the depressive ring around the core [μm]	3,00	3,00
Molar concentration of fluorine in the depressive ring around the core [M%]	1,0	1,0
Spacing between the core and the depressive ring around the core [μm]	4,95	4,95
Verdet constant $\left[\frac{\text{rad}}{\text{T} \cdot \text{m}} \right]$	4,3830	5,4635
The refractive index in the core	1,4513	1,4485
The refractive index in the cladding	1,4468	1,4440
The refractive index in the cladding depression	1,4421	1,4394
Cutoff wavelength [μm]	1,00	1,00

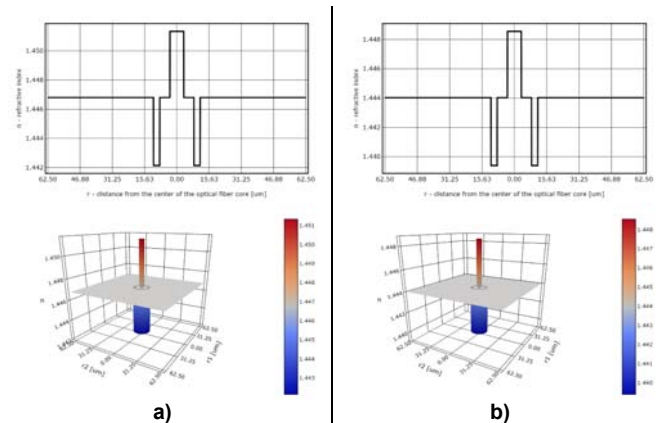


Fig. 9. The profile shapes of the refractive index in the core and the cladding of G.657B single mode optical fiber: **a)** plot 2D and 3D for 2nd optical window, **b)** plot 2D and 3D for 3rd optical window [own results]

Conclusions

From works [9,10,11] results, that single mode optical fibers, including telecommunications, can be used to build various types of current sensors, while in the study [12] it was shown, that multimode optical fiber, including telecommunications, can function as distributed temperature sensors.

This resulted in the need to create an original computer application, which can be used during design (property

modeling) single mode and multimode optical fibers with selected refractive index profiles, that can be used in the metrology of electric quantities (optical fiber current sensors) and non-electric (distributed temperature sensors).

In order to test the correctness of the application operation, a number of computer simulations were carried out. They consisted in the selection of the appropriate type of refractive index profile and the introduction of appropriate chemical (construction), geometric and propagation parameters. The results of the application are: the numerical form of the Verdet constant, the values of refractive indexes and the cut-off wavelength, as well as the two-dimensional (2D) and three-dimensional (3D) graphic form of the refractive index distribution (profile) depending on the distance from the core center (axis) of the optical fiber core.

It is worth noting here that the cut-off wavelength is important from the designer's point of view. On its basis, it is possible to determine for which wavelengths of the designed optical fiber is single mode or multimode, as described in [13]. The application allows you to designate what is its advantage. Thanks to this, the designer can correctly select the parameters of the fiber so that it can work with the appropriate source of laser light.

During the tests, the focus was on commonly available and used telecommunications optical fibers. Their catalog parameters are included in Table 3. ÷ 5. The obtained results (Table 6. ÷ 11.) were compared with the normative values of refractive indices, Verdet constant and cutoff wavelength (single mode and multimode) included in the papers [13,18]. The correct comparison results were obtained, which proves the correctness of the operation of this application.

Table 12. Geometric and transmission parameters of the photosensitive optical fiber PS-HNN-40 with a large numerical aperture

Core diameter [μm]	5.6±0.5
Core dopant	GeO ₂
Molecular concentration of germanium in the core [M%]	12
Numerical aperture	0.20±0.02
LP ₁₁ cutoff wavelength [nm]	1450±50
Mode-field diameter [μm]	6.5±1.0
Attenuation at 3 rd optical window [dB/km]	<3
Cladding mode offset [nm]	5
Cladding diameter [μm]	125±1
Coating diameter [μm]	250±2

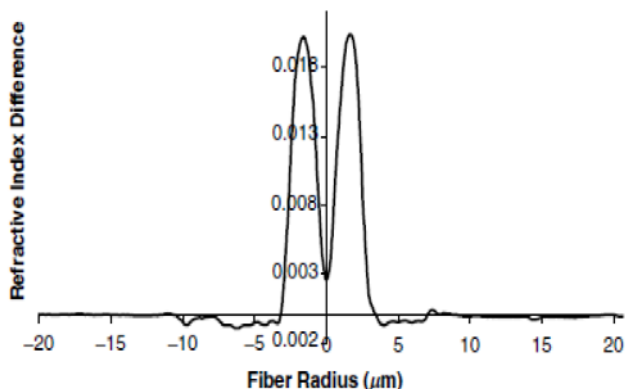


Fig. 10. The profile shapes refractive index in the core and the cladding of the photosensitive optical fiber PS-HNN-40 with a large numerical aperture

It is worth noting here, that the created application is characterized by very high accuracy, because it use mathematical formulas (with high precision of the result. It can therefore be used by engineers (designers) optical fiber

used in metrology of electrical and non-electrical quantities.

The computer application can be found at the link:

<https://michal037.github.io/tofma/tofma/>

In addition to telecommunication optical fibers, photosensitive optical fibers can be used to build optical fiber sensors of electrical and non-electrical quantities [25,26,27], which are currently becoming more and more popular on the optical fiber optoelectronics market. The photosensitivity of a medium is defined as its ability to have a completely changed physical and chemical refractive index of the medium by irradiation [28]. The group of these optical fibers includes, among others, standard single-mode fibers with hydrogenation, silicon-germanium fibers with boron doping, fibers with a large numerical aperture, i.e. with a core highly doped with germanium, and fibers with limited cladding transmission. Using the application presented in the work, apart from telecommunications optical fibers, it is also possible to design photosensitized fibers with a large numerical aperture, for which the value of the core refractive index can be completely changed by ultraviolet irradiation, and their geometrical and transmission parameters are included in Table 12. The profile shapes refractive index in the core and the cladding of the photosensitive optical with a large numerical aperture is shown in the Figure 10.

Authors: PhD Eng. Sławomir Andrzej Torbus, Associate Professor, Kazimierz Wielki University in Bydgoszcz, Institute of Mathematics, al. Powstańców Wielkopolskich 2, 85-090 Bydgoszcz, E-mail: slawomir.torbus@ukw.edu.pl; Eng. Michał Kozakiewicz, E-mail: michalkozakiewicz3@gmail.com;

REFERENCES

- [1] Opilski A., Czujniki Światłowodowe, I Krajowa Szkoła Optoelektroniki, Unieście (1987)
- [2] Tumański S., Czujniki pola magnetycznego – stan obecny i kierunki rozwoju, Przegląd Elektrotechniczny Nr 2 (2004)
- [3] Nakielna P., Czerwiec J., Czujniki magnetyczne wykorzystujące efekt Faradaya, Uniwersytet Jagielloński, Instytut Fizyki, Zakład Fotoniki, Kraków (2007)
- [4] Yariv A., Yeh P., Optical Waves in Crystals, JohnWiley & Sons, New York (1984)
- [5] Torbus S. A., Wpływ stężenia molowego domieszki GeO₂ w rdzeniu światłowodu wielomodowego na rozdzielczość temperaturową rozłożonego czujnika temperatury z wymuszonym rozproszeniem Ramana, Przegląd Elektrotechniczny Nr 3 (2019)
- [6] Torbus S. A., Tota J., Janikowski Ł., Optical fiber telemetry link to transmission of measuring signals, Przegląd Elektrotechniczny Nr 5 (2018)
- [7] Grattan K. T. V., Meggit B. T., Optical fiber sensor technology, Kluwer Academic Publisher, Bosto (2000)
- [8] Yu F. T. S., Yin S., Fiber optic sensors, Marcel Dekker Inc., New York (2002)
- [9] Torbus S.A., Zastosowanie światłowodów telekomunikacyjnych G.652, G.653 i G.655 w polarymetrycznych czujnikach natężenia prądu, Pomiary Automatyka Kontrola Nr 5 (2011)
- [10] Torbus S. A., Ratuszek M., Zastosowanie jednomodowych światłowodów telekomunikacyjnych odpornych na zginanie G.657 do realizacji cewki pomiarowej polarymetrycznego czujnika natężenia prądu, Przegląd Elektrotechniczny Nr 4a (2012)
- [11] Torbus S. A., Fajfer M., Ratuszek M. J., Projektowanie jednomodowych światłowodów telekomunikacyjnych odpornych na zginanie G.657 dla celów metrologicznych, Przegląd Elektrotechniczny Nr 8 (2013)
- [12] Torbus S. A., „Current – polarization-dependent loss” optical fibre sensor, Przegląd Elektrotechniczny Nr 5 (2019)
- [13] Majewski A., Teoria i projektowanie światłowodów, WNT, Warszawa (1991)
- [14] Shimosato M., Kozuka Y., Imaeda M., Magneto-optic Current Field Sensor with Sensivity Independent of Verdet Constant

- and Light Intensity, IEEE Translation Journal on Magnetic in Japan, Vol. 6, No. 5 (1991)
- [15] Ryaben'kii V. S., Tsynkov S. V., A Theoretical Introduction to Numerical Analysis, Chapman & Hall/CRC, Taylor & Francis Group (2007)
- [16] Snyder A. W., Love J. D., Optical waveguide theory, Izd. Radio i Swiaz, Moskwa (1987)
- [17] Romaniuk R., Szkło nieliniowe dla fotoniki. Część 5. Szkła Verdet – Faradaya, Elektronika nr 10 (2008)
- [18] Torbus S. A., Ratuszek M., The selection method of the single mode telecommunication fiber to the interferometric current sensor depending on the destination areas, Photonics Applications in Astronomy, Communications, Industry, and High-Energy Physics Experiments 2010, Proc. of SPIE, 0277-786X, Vol. 7745, 7745-81 (2010)
- [19] Marciniak M., Łączność światłowodowa, WKŁ, Warszawa (2002)
- [20] Perlicki K., Pomiar w optycznych systemach telekomunikacyjnych, WKŁ, Warszawa (2002)
- [21] Marcuse D., Theory of Dielectric Optical Waveguides, Academic Press, New York (1991)
- [22] Blake J. N., Rose A. H., Precision Fiber-Optic Current Sensor as a Check-Standard, IEEE 0-7803-7519-X/02 (2002)
- [23] Dawson J. W., MacDougall W., Hernandez E., Verdet Constant Limited Temperature Response of a Fiber-Optic Current Sensor, IEEE Photonic Technology Letters, Vol. 7, No. 12 (1995)
- [24] Torbus S. A., Możliwości termicznego łączenia światłowodów jednomodowych wykorzystywanych w metrologii, Przegląd Elektrotechniczny Nr 1 (2019)
- [25] Lindner E., Chojetzki Ch., Brückner S., Becker M., Rothhardt M., Bartelt H., Thermal regeneration of fiber Bragg gratings in photosensitive fibers, Optics Express, Vol. 17, Issue 15 (2009)
- [26] Fokine M., Photosensitivity, chemical composition gratings and optical fiber based components, KTH, Superseded Departments, Microelectronics and Information Technology, IMIT, Stockholm (2002)
- [27] Campbell R. J., Kashyap R., Spectral profile and multiplexing of Bragg gratings in photosensitive fiber, Optics Letters, Vol. 16, Issue 12 (1991)
- [28] Hill K. O., Fujii Y., Johnson D. C., Kawasaki B. S., Photosensitivity in optical fiber waveguides: Application to reflection filter fabrication, Applie Physics Letters, Vol. 32 (1978)